Acta Crystallographica Section F
Structural Biology and Crystallization Communications
ISSN 1744-3091

Expression, purification and crystallization of class C acid phosphatases from *Francisella tularensis* and *Pasteurella multocida*

Harkewal Singh,[a] Richard L. Felts,[a] Li Ma,[a] Thomas J. Malinski,[b] Michael J. Calcutt,[b] Thomas J. Reilly[b,c] and John J. Tanner[a,d]*

[a]Department of Chemistry, University of Missouri-Columbia, Columbia, MO 65211, USA, [b]Department of Veterinary Pathobiology, University of Missouri-Columbia, Columbia, MO 65211, USA, [c]Veterinary Medicine Diagnostic Laboratory, University of Missouri-Columbia, Columbia, MO 65211, USA, and [d]Department of Biochemistry, University of Missouri-Columbia, Columbia, MO 65211, USA

Correspondence e-mail: tannerjj@missouri.edu

Received 10 November 2008
Accepted 12 January 2009

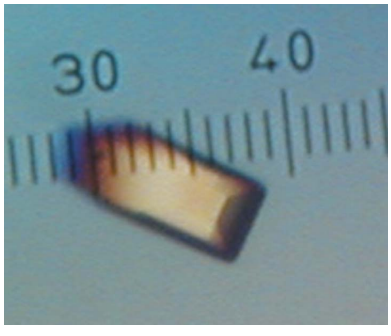

Class C nonspecific acid phosphatases are bacterial enzymes that are secreted across the cytoplasmic membrane and hydrolyze a variety of phosphomonoesters at acidic pH. These enzymes are of interest for the development of improved vaccines and clinical diagnostic methods. In one case, the category A pathogen *Francisella tularensis*, the class C phosphatase plays a role in bacterial fitness. Here, the cloning, expression, purification and crystallization methods for the class C acid phosphatases from *F. tularensis* and *Pasteurella multocida* are reported. Crystals of the *F. tularensis* enzyme diffracted to 2.0 Å resolution and belonged to space group $C222_1$, with one enzyme molecule in the asymmetric unit. Crystals of the *P. multocida* enzyme diffracted to 1.85 Å resolution and belonged to space group *C*2, with three molecules in the asymmetric unit. Diffraction patterns from crystals of the *P. multocida* enzyme exhibited multiple interpenetrating reciprocal-space lattices, indicating epitaxial twinning. Despite this aberrance, autoindexing was robust and the data could be satisfactorily processed to 1.85 Å resolution using *MOSFLM* and *SCALA*.

1. Introduction

Acid phosphatases (EC 3.1.3.2) are ubiquitous and catalyze the transfer of phosphoryl groups from phosphomonoesters to water at acidic pH (Vincent *et al.*, 1992). They play essential roles in the generation, acquisition and mobilization of inorganic phosphate, as well as critical roles in the phosphoryl relay systems involved in signal transduction pathways in both prokaryotes and eukaryotes.

Three classes of bacterial nonspecific acid phosphatases (NSAPs) have been identified (denoted A, B and C) based on subcellular localization and conserved amino-acid sequence motifs (Rossolini *et al.*, 1998). The enzymes studied here belong to class C, which is characterized by the presence of four invariant aspartate residues known as the DDDD motif (in bold) contained within the bipartite signature motif (I/V)-(V/A/L)-**D**-(I/L)-**D**-E-T-(V/M)-L-*X*-(N/T)-*X*-*X*-Y near the N-terminus and (I/V)-(L/M)-*X*-*X*-G-**D**-(N/T)-L-*X*-**D**-F near the C-terminus (Thaller *et al.*, 1998). Several class C enzymes have been purified and/or characterized, including those from *Haemophilus influenzae* [known as *e* (P4); Reilly *et al.*, 1999; Reilly & Smith, 1999], *Bacillus anthracis* (Felts *et al.*, 2006), *Streptococcus equisimilis* (Malke, 1998), *Staphylococcus aureus* (du Plessis *et al.*, 2002), *Helicobacter pylori* (Reilly & Calcutt, 2004), *Chryseobacterium meningosepticum* (Passariello *et al.*, 2003) and *Clostridium perfringens* (Reilly *et al.*, 2009). Shared attributes include a polypeptide size of 25–30 kDa, a requirement for metal cation for catalytic activity and rather broad substrate specificity. Most have an N-terminal lipidated Cys that anchors them to the outer membrane of the bacterium. The *S. aureus* and *C. perfringens* enzymes appear to be exceptions in this respect.

The crystal structures of the class C NSAPs from *H. influenzae* (Felts *et al.*, 2007; Ou *et al.*, 2006) and *B. anthracis* (PDB code 2i33) have been determined. The structures show that class C NSAPs belong to the haloacid dehalogenase structural superfamily and that

the conserved Asp residues of the DDDD motif participate in binding an active-site Mg^{2+} ion (Felts *et al.*, 2007). Furthermore, the structure of the *H. influenzae* enzyme complexed with a tungstate-ion inhibitor suggests that the first Asp of the motif is the nucleophile that attacks the substrate P atom (Felts *et al.*, 2007).

There is emerging interest in class C NSAPs. Because of their localization to the bacterial outer membrane, they are potentially attractive candidates for vaccine development. In fact, significant progress has been made towards creating a vaccine against non-typeable *H. influenzae* using catalytically inactive mutants of recombinant *e* (P4) (Hotomi *et al.*, 2005; Mason *et al.*, 2004; Green *et al.*, 2005). Moreover, the class C NSAP from the category A bioterrorism pathogen *Francisella tularensis* has been implicated in phagosomal escape and virulence (Mohapatra *et al.*, 2008). Finally, detection of acid phosphatase activity is a useful diagnostic tool for the clinical identification of *C. perfringens* (Adcock & Saint, 2001; Eisgruber *et al.*, 2003; Sartory *et al.*, 2006). Presumably, these methods detect the *Clostridium* class C NSAP. By extension, it may be possible to develop analogous tools for the identification of other bacteria based on immunological and biochemical detection of an organism's unique class C NSAP. Elucidation of the crystal structures of class C NSAPs will aid this effort.

To facilitate further investigations of this enzyme family, we have developed recombinant expression systems for the class C enzymes from *F. tularensis* (FtAcpC) and *Pasteurella multocida* (PmAcpC), the latter being a pathogen of significant agricultural importance (Harper *et al.*, 2006). Methods for expressing, purifying and crystallizing these enzymes are described here, together with preliminary analyses of their X-ray diffraction data.

2. Methods and results

2.1. Cloning of the *FtAcpC* gene

The *FtAcpC* gene has been identified previously as one of five phosphatase genes present in the genome sequence of *F. tularensis* subsp. *novicida* (Mohapatra *et al.*, 2008). The gene encodes a 247-residue protein that has 25% identity over 225 amino acids to *H. influenzae e* (P4), the archetype of class C NSAPs. Moreover, the sequence contains a bipartite motif that is characteristic of class C NSAPs. The motif for FtAcpC is IL**D**I**D**ETALDNS at residues 73–84 followed by IAYFG**D**NIQ**D**F at residues 202–212. Secretion across the cytoplasmic membrane is a defining characteristic of class C NSAPs, so the protein sequence was analyzed for potential signal peptides. Analysis using the *SignalP* 3.0 (Bendtsen *et al.*, 2004), *SignalBLAST* (Frank & Sippl, 2008) and *PSORT* 6.4 (Nakai & Kanehisa, 1991) servers suggests that the N-terminus contains a signal peptide of 20–23 residues in length, implying that the protein is expressed as a precursor polypeptide that is exported from the cytoplasm and cleaved to yield the mature enzyme. There is a cysteine at position 24 which could potentially be lipidated, as is predicted for most other class C NSAPs, but this remains to be determined. The sequence similarity to *e* (P4), the bipartite DDDD motif and the predicted export from the cytoplasm are consistent with classification of the enzyme into the class C NSAP family.

The *FtAcpC* gene (NCBI RefSeq No. YP_169641) was cloned from genomic DNA of *F. tularensis* strain SCHU S4 (Larsson *et al.*, 2005). The gene was amplified by PCR and inserted into pET20b using *Nco*I and *Xho*I restriction sites. To avoid potential problems with membrane association, the N-terminal 24 residues were replaced by the *pelB* leader sequence followed by Met-Gly. Thus, the mature recombinant enzyme expressed in *Escherichia coli* is exported to the periplasmic space and is predicted to have N-terminal residues MGNSVNI and a C-terminal His_6 tag.

2.2. Identification and cloning of the *PmAcpC* gene

A query of the complete genome sequence of *P. multocida* strain Pm70 (May *et al.*, 2001) with class C NSAP genes identified an open reading frame, designated PM1064, which had the potential to be a class C NSAP. PM1064 encodes 272 residues having 59% global amino-acid sequence identity to *e* (P4). PmAcpC contains a classic 19-residue lipoprotein signal peptide at the N-terminus (Hayashi & Wu, 1990). The predicted signal peptide contains positively charged residues (Lys) at positions −18 and −15, followed by a hydrophobic region and ending in the lipoprotein box LLAA-C. Thus, the mature form of PmAcpC is predicted to be a 253-residue lipoprotein with Cys1 modified by lipidation. Furthermore, the predicted protein contains a class C bipartite sequence motif VV**D**L**D**ETMIDNS at residues 61–72 of the mature protein and VLFVG**D**NLN**D**F at residues 175–185. The high sequence identity with *e* (P4), the bipartite DDDD motif and lipoprotein prediction are consistent with assignment of this protein as a class C NSAP.

The *PmAcpC* gene (GenBank accession No. FJ609981) was cloned from genomic DNA from a clinical isolate. The gene was amplified by PCR and cloned as an *Nco*I–*Xho*I fragment into pET20b. To produce soluble protein in *E. coli*, the N-terminal 20 residues were replaced by the *pelB* leader sequence followed by Met-Val. The mature recombinant enzyme is thus exported to the periplasmic space and is predicted to have N-terminal residues MVSNQQA and a C-terminal His_6 tag.

2.3. Expression and purification of FtAcpC

Recombinant FtAcpC was expressed in *E. coli* BL21 (DE3). A starter culture was grown overnight at 310 K in 5 ml LB supplemented with 50 µg ml^{-1} ampicillin and 0.2%(*w*/*v*) glucose. The starter culture was diluted 1:500 into 35 ml LB containing 50 µg ml^{-1} ampicillin and 0.2%(*w*/*v*) glucose. The culture was incubated at 310 K with constant aeration supplied by orbital shaking at 250 rev min^{-1} until the OD_{600} reached 0.6. The cells were then centrifuged at 277 K (3600*g* for 10 min) and the resulting pellet was resuspended in 4 ml LB and diluted 1000-fold into 1 l LB containing 50 µg ml^{-1} ampicillin and 0.2%(*w*/*v*) glucose. The culture was incubated at 310 K with constant aeration (250 rev min^{-1}) and induced with 0.4 m*M* IPTG when the OD_{600} reached 0.4. The incubation was continued at the lower temperature of 298 K and with a decreased shaking rate of 220 rev min^{-1} until the OD_{600} reached 1.0. The cells were harvested by centrifugation (3600*g*, 277 K), suspended in 50 m*M* Tris–HCl pH 8.4 and frozen.

The frozen cell suspension was thawed and the cells were disrupted in a Thermo 40K cell French Press adjusted to 69 MPa for two cycles at a low flow rate to maintain the cell pressure. Unbroken cells and cellular debris were removed by centrifugation at 31 000*g* for 20 min at 277 K. Remaining bacterial membranes were pelleted by centrifugation at 183 960*g* for 1 h at 277 K.

The supernatant from ultracentrifugation was filtered through a 0.2 µm Millipore filter and applied onto a Q Sepharose anion-exchange column with an ÄKTA FPLC chromatography system. The sample was loaded onto the column at 2 ml min^{-1} using a buffer of 50 m*M* Tris–HCl pH 8.4. A linear NaCl gradient was then applied, eluting FtAcpC in the range 60–100 m*M* NaCl. Fractions containing FtAcpC were identified using SDS–PAGE and phosphatase-activity assays, the latter consisting of a discontinuous colorimetric assay using *p*-nitrophenylphosphate as the substrate (Reilly *et al.*, 2006).

The pooled fractions were dialyzed overnight at 277 K against 20 m*M* phosphate buffer pH 7.0 containing 0.5 *M* NaCl in preparation for immobilized metal-ion affinity chromatography. The dialyzed sample was loaded onto an Ni^{2+}-charged affinity column and eluted with 175–200 m*M* imidazole. Fractions having the highest purity level, based on SDS–PAGE, were pooled and dialyzed overnight into 50 m*M* sodium acetate buffer pH 6.0. Finally, the sample was concentrated to 10 mg ml^{-1} using a centrifugal concentrating device. Protein concentration was assessed using the BCA method (Pierce kit).

2.4. Expression and purification of PmAcpC

Recombinant PmAcpC was expressed using the auto-induction method (Studier, 2005). A single colony of *E. coli* BL21 (DE3) containing the engineered plasmid was used to inoculate 5 ml LB containing ampicillin (50 µg ml^{-1}) and incubated overnight at 310 K. The culture was pelleted at 3660*g* and suspended in fresh LB prior to inoculation of four 2.8 l flasks, each containing 500 ml TY broth supplemented with the ZYM-5052 media components and ampicillin (50 µg ml^{-1}). The culture was grown with constant aeration at 310 K overnight.

The enzyme was purified using standard nondenaturing methods. All procedures were conducted at 277 K unless noted otherwise. Cultures from auto-induction were centrifuged at 3660*g* for 20 min and the pellet was suspended in 40 ml pH 7.0 buffer containing 20 m*M* sodium phosphate and 0.5 *M* NaCl. The suspension was stored at 253 K overnight and thawed the next day. A protease-inhibitor tablet (SigmaFAST) and DNase were added to the thawed suspension and mixed for approximately 30 min. The cells were disrupted and subjected to low-speed centrifugation and ultracentrifugation steps as described above for FtAcpC. The ultracentrifugation supernatant was retained and refrigerated.

The supernatant from ultracentrifugation was loaded at 2 ml min^{-1} onto a 5 ml Ni^{2+}-charged HiTrap metal-chelate chromatography resin using an ÄKTAprime system. The resin was washed with 20 m*M* sodium phosphate, 0.5 *M* NaCl, 50 m*M* imidazole pH 7.0 until the A_{280} returned to baseline. A 200 ml linear imidazole gradient (0.05–2.0 *M* imidazole in 20 m*M* sodium phosphate pH 7.0, 0.5 *M* NaCl) was applied and the eluate was collected in 2 ml fractions. PmAcpC eluted at approximately 200 m*M* imidazole. Fractions containing high phosphatase activity (*p*-nitrophenylphosphate substrate) were pooled and dialyzed overnight against 50 m*M* sodium acetate pH 6.0.

The dialyzed sample was loaded at a flow rate of 2.0 ml min^{-1} onto a 5 ml SP-Sepharose cation-exchange column that had been equilibrated with 50 m*M* sodium acetate pH 6.0. The column was washed with 50 m*M* sodium acetate pH 6.0 until the A_{280} returned to baseline. The phosphatase was eluted from the column with a 200 ml linear NaCl gradient (0.0–1.0 *M*) and collected in 2 ml fractions. PmAcpC eluted in the range 0.44–0.53 *M* NaCl. Enzymatically active fractions that were judged to be highly pure by SDS–PAGE were pooled and dialyzed overnight against 20 m*M* sodium phosphate pH 7.0. The sample was then concentrated to 10 mg ml^{-1} (BCA assay) using a 10 000 molecular-weight cutoff Centricon filtering device.

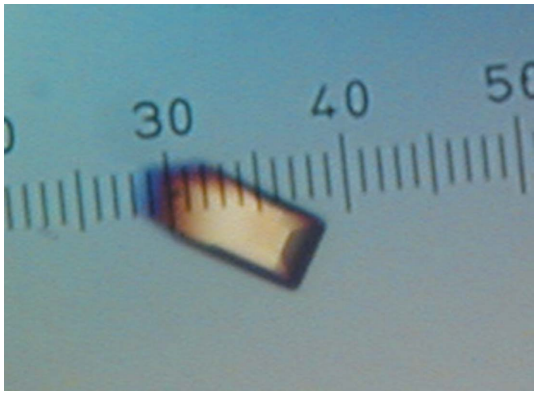

Figure 1
A crystal of FtAcpC. The smallest dimension of the ruler corresponds to 20 µm.

Table 1
Data-processing statistics for FtAcpC.

Values in parentheses are for the outermost resolution shell.

Space group	$C222_1$
Wavelength (Å)	0.97909
Unit-cell parameters (Å)	a = 59.2, b = 124.2, c = 62.2
Protein molecules in ASU	1
V_M (Å^3 Da^{-1})	2.3
Solvent content (%)	46
Resolution (Å)	27.8–2.00 (2.11–2.00)
Total observations	70800
Unique reflections	15842
Redundancy	4.5 (4.0)
Completeness (%)	99.8 (99.1)
Mean $I/\sigma(I)$	16.3 (3.8)
R_{merge}†	0.073 (0.470)
R_{merge}† in low-resolution bin	0.034

† $R_{merge} = \sum_{hkl}\sum_i |I_i(hkl) - \langle I(hkl)\rangle| / \sum_{hkl}\sum_i I_i(hkl)$, where $I_i(hkl)$ is the ith observation of reflection hkl and $\langle I(hkl)\rangle$ is the weighted average intensity for all observations of reflection hkl.

2.5. Crystallization of FtAcpC and preliminary analysis of X-ray diffraction data

Crystallization trials were performed at 293 K using the sitting-drop method of vapor diffusion with Cryschem plates and reservoir volumes of 1 ml. Drops were formed by mixing 2 µl protein stock solution and 2 µl reservoir solution. Crystal screening trials using commercially available reagent kits revealed promising crystallization conditions consisting of 25–30%(*w*/*v*) PEG 3350, 0.1 *M* bis-tris pH 5.5–6.5 and 0.1–0.2 *M* of either sodium chloride or ammonium acetate. The latter salt proved to be the preferred additive and eventually the best crystals were grown using reservoir solutions consisting of 24–32%(*w*/*v*) PEG 3350, 0.1 *M* bis-tris pH 6.5 and 0.1 *M* ammonium acetate. The optimized crystals appeared as rectangular blocks with a maximum dimension of approximately 0.2 mm (Fig. 1).

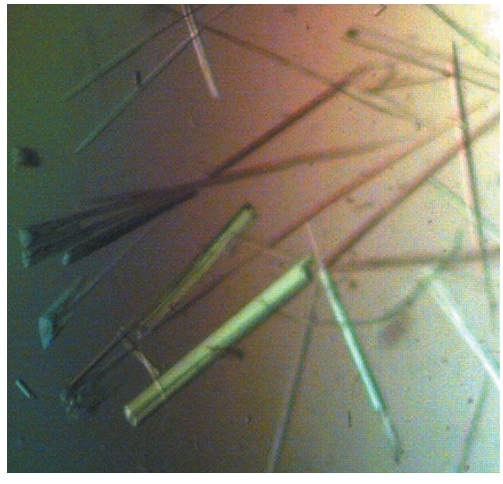

Figure 2
Crystals of PmAcpC. Note that the crystals grow as clusters of needles. The thickest clusters are approximately 20–40 µm thick.

In preparation for low-temperature data collection, the crystals were soaked in 30%(*w*/*v*) PEG 3350, 0.1 *M* bis-tris pH 6.5, 0.1 *M* ammonium acetate and 20%(*v*/*v*) PEG 200. The cryoprotected crystals were picked up with Hampton loops and plunged into liquid nitrogen.

FtAcpC crystals were analyzed on Advanced Light Source beamline 4.2.2 using a NOIR-1 CCD detector. Autoindexing calculations with *d*TREK* (Pflugrath, 1999) and *MOSFLM* (Leslie, 1992, 2006) indicated a *C*-centered orthorhombic lattice with unit-cell parameters a = 59.2, b = 124.2, c = 62.2 Å. Using the method of Matthews (Matthews, 1968; Kantardjieff & Rupp, 2003), the asymmetric unit is predicted to contain one FtAcpC molecule and 46% solvent. A data set consisting of 115 frames was collected with a crystal-to-detector distance of 150 mm, an oscillation width of 1.0° per frame and an exposure time of 5 s per frame. The data set was integrated with *MOSFLM* through the *iMosflm* graphical interface and scaled to 2.0 Å resolution with *SCALA* (Evans, 2006) using the *CCP*4*i* interface (Potterton *et al.*, 2003). Data-processing statistics are listed in Table 1.

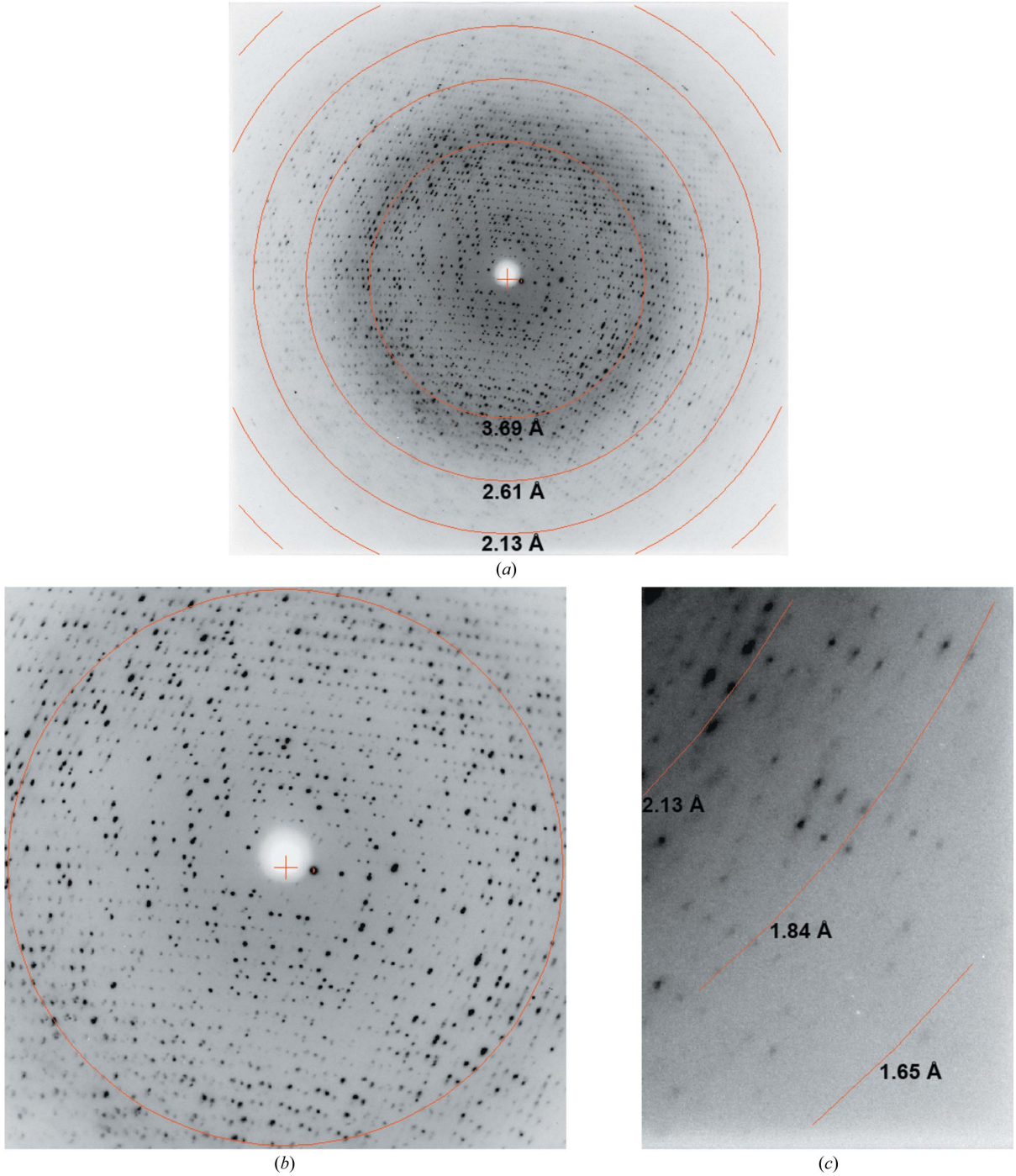

(*a*) (*b*) (*c*)

Figure 3
Diffraction image collected from a PmAcpC crystal. (*a*) Entire resolution range. (*b*) Enlarged view of the low-resolution region. The circle corresponds to 3.69 Å resolution. (*c*) Enlarged view of the high-resolution data.

Table 2
Data-processing statistics for PmAcpC.

Values in parentheses are for the outermost resolution shell.

Space group	*C*2
Wavelength (Å)	1.00000
Unit-cell parameters (Å, °)	a = 80.0, b = 106.1, c = 89.7, β = 93.1
Protein molecules in ASU	3
V_M (Å^3 Da^{-1})	2.2
Solvent content (%)	45
Resolution (Å)	27.5–1.85 (1.95–1.85)
Total observations	215684
Unique reflections	62294
Redundancy	3.5 (2.5)
Completeness (%)	97.8 (86.7)
Mean $I/\sigma(I)$	10.4 (3.1)
R_{merge}†	0.094 (0.272)
R_{merge}† in low-resolution bin	0.065

† $R_{merge} = \sum_{hkl}\sum_i |I_i(hkl) - \langle I(hkl)\rangle| / \sum_{hkl}\sum_i I_i(hkl)$, where $I_i(hkl)$ is the ith observation of reflection hkl and $\langle I(hkl)\rangle$ is the weighted average intensity for all observations of reflection hkl.

2.6. Crystallization of PmAcpC and preliminary analysis of X-ray diffraction data

Crystallization trials were performed at 293 K using the sitting-drop method (Cryschem plates, 1 ml reservoir volume) with drops formed by mixing 5 µl protein stock solution and 5 µl reservoir solution. Initial crystal screening trials revealed several promising conditions with PEG as the precipitating agent. The crystals invariably appeared as clusters of needles and although extensive optimization trials reduced the degree of fusion, it was not possible to grow truly single crystals. For example, the best crystals, which were grown using a reservoir solution of 20%(*w*/*v*) PEG 3350, 0.2 *M* ammonium citrate dibasic and 10%(*v*/*v*) *n*-propanol, still exhibited significant clustering and needle-like morphology (Fig. 2). In preparation for low-temperature data collection, the crystals were soaked in 25%(*w*/*v*) PEG 3350, 0.2 *M* ammonium citrate dibasic and 25%(*v*/*v*) PEG 200. The clusters were teased apart with Hampton loops in an attempt to isolate single crystals for data collection. The cryoprotected crystals were then plunged into liquid nitrogen.

X-ray diffraction data were collected on Advanced Light Source beamline 4.2.2 using a NOIR-1 CCD detector. The diffraction images clearly exhibited multiple interpenetrating reciprocal-space lattices (Fig. 3*a*), particularly at low resolution (Fig. 3*b*). The interpenetrating reciprocal lattices are symptomatic of epitaxial twinning and arise from multiple real-space lattices in the sample that are not perfectly aligned (Yeates & Fam, 1999; Chandra *et al.*, 1999). The crystals diffracted to surprisingly high resolution despite being rather thin. As shown in Fig. 3(*c*), reflections extending beyond 1.84 Å resolution were observed. Despite the epitaxial twinning, autoindexing using either *d*TREK* (Pflugrath, 1999) or *MOSFLM* was robust and consistently indicated *C*2 as the space group, with unit-cell parameters a = 80.0, b = 106.1, c = 89.7 Å, β = 93.1°. The assumption of three PmAcpC molecules in the asymmetric unit implies 45% solvent content and V_M = 2.2 Å^3 Da^{-1} (Matthews, 1968; Kantardjieff & Rupp, 2003).

A data set consisting of 360 frames was collected with an oscillation width of 0.5° per frame and a crystal-to-detector distance of 140 mm. Integration was performed with *MOSFLM* through the *iMosflm* interface and scaling calculations were performed with *SCALA via CCP4i*. The data could be processed satisfactorily to 1.85 Å resolution, as shown in Table 2. Note, however, that R_{merge} is 0.065 in the low-resolution bin, which is rather high. Presumably, this suboptimal result is a consequence of the presence of multiple reciprocal-space lattices, which are particularly evident at low resolution (Fig. 3*b*). For comparison, R_{merge} is 0.034 in the low-resolution bin for the FtAcpC data (Table 1).

We thank Dr Jay Nix of ALS beamline 4.2.2 for assistance with data collection and Dr Fran Nano for providing the *F. tularensis* DNA used for cloning. HS was supported by a pre-doctoral fellowship from National Institutes of Health grant DK071510. This research was supported by National Institutes of Health grant U54-AI057160 to the Midwest Regional Center of Excellence for Biodefense and Emerging Infectious Diseases Research (to JJT and TJR), the University of Missouri Research Board (to JJT and TJR) and the Program for Prevention of Animal Infectious Diseases USDA ARS 58-1940-5-519 (to TJR and MJC). Part of this work was performed at the Advanced Light Source, which is supported by the Director, Office of Science, Office of Basic Energy Sciences of the US Department of Energy under Contract No. DE-AC02-05CH11231.

References

Adcock, P. W. & Saint, C. P. (2001). *Appl. Environ. Microbiol.* **67**, 4382–4384.
Bendtsen, J. D., Nielsen, H., von Heijne, G. & Brunak, S. (2004). *J. Mol. Biol.* **340**, 783–795.
Chandra, N., Acharya, K. R. & Moody, P. C. E. (1999). *Acta Cryst.* D**55**, 1750–1758.
Eisgruber, H., Geppert, P., Sperner, B. & Stolle, A. (2003). *Int. J. Food Microbiol.* **82**, 81–86.
Evans, P. (2006). *Acta Cryst.* D**62**, 72–82.
Felts, R. L., Ou, Z., Reilly, T. J. & Tanner, J. J. (2007). *Biochemistry*, **46**, 11110–11119.
Felts, R. L., Reilly, T. J., Calcutt, M. J. & Tanner, J. J. (2006). *Acta Cryst.* F**62**, 705–708.
Frank, K. & Sippl, M. J. (2008). *Bioinformatics*, **24**, 2172–2176.
Green, B. A., Baranyi, E., Reilly, T. J., Smith, A. L. & Zlotnick, G. W. (2005). *Infect. Immun.* **73**, 4454–4457.
Harper, M., Boyce, J. D. & Adler, B. (2006). *FEMS Microbiol. Lett.* **265**, 1–10.
Hayashi, S. & Wu, H. C. (1990). *J. Bioenerg. Biomembr.* **22**, 451–471.
Hotomi, M., Ikeda, Y., Suzumoto, M., Yamauchi, K., Green, B. A., Zlotnick, G., Billal, D. S., Shimada, J., Fujihara, K. & Yamanaka, N. (2005). *Vaccine*, **23**, 1294–1300.
Kantardjieff, K. A. & Rupp, B. (2003). *Protein Sci.* **12**, 1865–1871.
Larsson, P. *et al.* (2005). *Nature Genet.* **37**, 153–159.
Leslie, A. G. W. (1992). *Jnt CCP4–ESF/EACBM Newsl. Protein Crystallogr.* **26**.
Leslie, A. G. W. (2006). *Acta Cryst.* D**62**, 48–57.
Malke, H. (1998). *Appl. Environ. Microbiol.* **64**, 2439–2442.
Mason, K. W., Zhu, D., Scheuer, C. A., McMichael, J. C., Zlotnick, G. W. & Green, B. A. (2004). *Vaccine*, **22**, 3449–3456.
Matthews, B. W. (1968). *J. Mol. Biol.* **33**, 491–497.
May, B. J., Zhang, Q., Li, L. L., Paustian, M. L., Whittam, T. S. & Kapur, V. (2001). *Proc. Natl Acad. Sci. USA*, **98**, 3460–3465.
Mohapatra, N. P., Soni, S., Reilly, T. J., Liu, J., Klose, K. E. & Gunn, J. S. (2008). *Infect. Immun.* **76**, 3690–3699.
Nakai, K. & Kanehisa, M. (1991). *Proteins*, **11**, 95–110.
Ou, Z., Felts, R. L., Reilly, T. J., Nix, J. C. & Tanner, J. J. (2006). *Acta Cryst.* F**62**, 464–466.
Passariello, C., Schippa, S., Iori, P., Berlutti, F., Thaller, M. C. & Rossolini, G. M. (2003). *Biochim. Biophys. Acta*, **1648**, 203–209.
Pflugrath, J. W. (1999). *Acta Cryst.* D**55**, 1718–1725.
Plessis, E. M. du, Theron, J., Joubert, L., Lotter, T. & Watson, T. G. (2002). *Syst. Appl. Microbiol.* **25**, 21–30.
Potterton, E., Briggs, P., Turkenburg, M. & Dodson, E. (2003). *Acta Cryst.* D**59**, 1131–1137.
Reilly, T. J. & Calcutt, M. J. (2004). *Protein Expr. Purif.* **33**, 48–56.
Reilly, T. J., Chance, D. L., Calcutt, M. J., Tanner, J. J., Felts, R. L., Waller, S. C., Henzl, M. T., Mawhinney, T. P., Ganjam, I. K. & Fales, W. H. (2009). Submitted.
Reilly, T. J., Chance, D. L. & Smith, A. L. (1999). *J. Bacteriol.* **181**, 6797–6805.
Reilly, T. J., Felts, R. L., Henzl, M. T., Calcutt, M. J. & Tanner, J. J. (2006). *Protein Expr. Purif.* **45**, 132–141.
Reilly, T. J. & Smith, A. L. (1999). *Protein Expr. Purif.* **17**, 401–409.

Rossolini, G. M., Schippa, S., Riccio, M. L., Berlutti, F., Macaskie, L. E. & Thaller, M. C. (1998). *Cell. Mol. Life Sci.* **54**, 833–850.
Sartory, D. P., Waldock, R., Davies, C. E. & Field, A. M. (2006). *Lett. Appl. Microbiol.* **42**, 418–424.
Studier, F. W. (2005). *Protein Expr. Purif.* **41**, 207–234.
Thaller, M. C., Schippa, S. & Rossolini, G. M. (1998). *Protein Sci.* **7**, 1647–1652.
Vincent, J. B., Crowder, M. W. & Averill, B. A. (1992). *Trends Biochem. Sci.* **17**, 105–110.
Yeates, T. O. & Fam, B. C. (1999). *Structure Fold. Des.* **7**, R25–R29.